An Adiabatic Linearized Path Integral Approach for Quantum Time Correlation Functions: Electronic Transport in Metal−Molten Salt Solutions†

Maria Serena Causo and Giovanni Ciccotti

Dipartimento di Fisica, Università "La Sapienza", Piazzale Aldo Moro, 2, 00185 Roma, Italy

Daniel Montemayor, Sara Bonella, and David F. Coker*

Department of Chemistry, Boston University, 590 Commonwealth Avenue, Boston, Massachusetts 02215

Received: October 20, 2004; In Final Form: December 5, 2004

We generalize the linearized path integral approach to evaluate quantum time correlation functions for systems best described by a set of nuclear and electronic degrees of freedom, restricting ourselves to the adiabatic approximation. If the operators in the correlation function are nondiagonal in the electronic states, then this adiabatic linearized path integral approximation for the thermal averaged quantum dynamics presents interesting and distinctive features, which we derive and explore in this paper. The capability of these approximations to accurately reproduce the behavior of physical systems is demonstrated by calculating the diffusion constant for an excess electron in a metal−molten salt solution.

Introduction

The evaluation of thermal averaged time correlation functions is a challenging and important aspect of many problems in chemistry and physics. Through linear response theory, these quantities can describe relaxation processes for systems not too far from equilibrium; they are also a crucial element in linking the behavior of microscopic properties to macroscopic transport coefficients via the Green−Kubo relations. Because of this significance, much effort has been devoted in recent years to calculating quantum time correlation functions for physical systems of increasing complexity. Since the full quantum problem is, in general, still too expensive to be addressed exactly, numerous approximation techniques have been developed for the simulation of systems where quantum mechanical aspects of the dynamics are important. Among these techniques, the semiclassical initial value representation, in its linearized version,[1−6] has proved quite successful in obtaining, for example, flux−flux correlation functions related to chemical reaction rates. Recently Poulsen, Nyman, and Rossky[7,8] and independently Shi and Geva[9−12] have shown how linearized semiclassical expressions for thermal averaged time correlation functions can be obtained directly from exact path integral forms. The result they obtain has also emerged in the literature as an approximation to the time evolution of the Wigner equivalent of the quantum time correlation function.[13] However they are derived, these approximate expressions for thermal averaged time correlation functions have the appealing feature of requiring only two main ingredients for their calculation: a set of initial conditions sampled from a quantity related to the Wigner representation of the thermal density matrix and the corresponding set of classically evolved trajectories. Calculating the Wigner transformation of the thermal density operator is a highly nontrivial problem for anharmonic systems, but the method proposed by Poulsen and co-workers and a related approach presented by Shi and Geva[11,12] provide viable procedures to accomplish this goal. Poulsen and co-workers, for example, have recently applied their version of the linearized path integral method to the calculation of the intermediate scattering function for helium in the quantum regime.[8]

In this paper, we generalize the linearized path integral approach to situations in which the system needs to be described in terms of a set of nuclear degrees of freedom evolving in the presence of several electronic states. This might be the case when studying processes involving electronic transitions that occur as a result of coupled nuclear and electronic dynamics (nonadiabatic processes). As we shall see in more detail in the next section, it is also the framework necessary to evaluate correlation functions of operators which are nondiagonal in the chosen electronic basis set.

An interesting example where this generalization is necessary is the study of the diffusion of an excess electron in a metal−molten salt solution. This problem has been addressed in the past by Selloni and co-workers[14] using a simulation method that restricts the dynamics of the ions on the electronic ground state and defines ad hoc estimators for the electronic diffusion that are in good agreement with experiments.[15] Therefore, this system provides an ideal benchmark to assess the performance of the new method.

The paper is organized as follows. In section 2, we start from a general, fully quantum expression for a thermal averaged time correlation function of operators of a quantum subsystem moving under the influence of a fluctuating environment. Such functions have the form

$$\langle \hat{A}\cdot\hat{B}(t)\rangle = \mathrm{Tr}\{\hat{\rho}\hat{A}\hat{U}^{\dagger}(t)\hat{B}\hat{U}(t)\} \qquad (1)$$

where $\hat{\rho} = \exp[-\beta\hat{H}]/Z$ is the normalized Boltzmann density operator with $Z = \mathrm{Tr}\exp[-\beta\hat{H}]$, $\hat{U}(t)$ is the full quantum propagator of the system, and we choose $\hat{A}$ and $\hat{B}$ to be operators of the electronic subsystem. We use the adiabatic basis states of the quantum subsystem to identify the contributions to the quantity defined in eq 1 coming from the density matrix and

* Author to whom correspondence should be addressed. Phone: (617) 353-2490. Fax: (617) 353-6466. E-mail: coker@bu.edu.

† Part of the special issue "David Chandler Festschrift".

10.1021/jp045208b CCC: $30.25
Published on Web 01/25/2005

the propagators and those relative to the matrix elements of the observables. We then write the propagators and the density matrix in terms of discrete path integrals and show in some detail how nonadiabatic effects arise in the chosen representation. This analysis allows us to appreciate the nature of the terms that are neglected when restricting, as we shall ultimately do in this paper, the quantum nuclear time evolution resulting from a given propagator ($\hat{U}$ or its hermitian conjugate) to a single electronic state in the spirit of the Born−Oppenheimer approximation. An approximate form of the quantum time correlation function based on the linearization of the propagators in a suitable set of variables will then be obtained and used together with a high-temperature approximation for the density matrix to derive an expression that can be calculated by sampling a set of initial conditions from an approximate Wigner transformed density matrix and propagating classical trajectories. The nature of the classical trajectories, however, is quite different from the prescription by Poulsen, Nyman, and Rossky.[7] In particular, we find that the final result is obtained by summing two types of contributions to the time correlation function. Those corresponding to diagonal elements of the operator in the specified basis imply propagation under forces determined by a single electronic eigenstate. The contributions from off-diagonal elements of operators, however, must be calculated using trajectories in which the nuclear variables move under the influence of the mean of two adiabatic surfaces determined by the specific matrix element of the operator that is being evaluated. Such contributions must also be weighted by a phase factor related to the energy gap between the states.

In section 3, we present results using these methods to explore the dynamics of an excess electron in a metal−molten salt solution and apply our approach to studying the system explored by Selloni and co-workers in ref 14. The simulations are performed at two different temperatures to investigate the effects of different thermodynamic conditions on the characteristics of the nuclear motion, with the specific aim to address the validity of the hypothesis of adiabatic nuclear motion on the ground state over a range of conditions. We then show how the new method presented in this work can be used to calculate the diffusion of the excess electron using estimators based on either the position or the velocity of the quantum particle, and we compare our results with those of previous calculations and experiments.

2. Theory: Adiabatic Correlation Functions

The aim of the discussion below is to perform a series of approximations to the quantum average in eq 1 that will ultimately allow us to express it in terms of appropriate combinations of classical objects that can be evaluated by computer simulation. To this end, we begin by using a standard representation in which the quantum subsystem (e.g., an electron) is described by a complete set of states and the environment (a set of nuclear degrees of freedom in our example) is described using the continuous coordinate representation. We choose to evaluate the trace in eq 1 using the adiabatic electronic states at nuclear configuration R that satisfy $H_{el}(R)|\Phi_i(R)\rangle = E_i(R)|\Phi_i(R)\rangle$ thus

$$\langle \hat{A}\cdot\hat{B}(t)\rangle = \sum_i \int \mathrm{d}R\, \langle R\Phi_i(R)|\hat{\rho}\hat{A}\hat{U}^{\dagger}(t)\hat{B}\hat{U}(t)|R\Phi_i(R)\rangle \tag{2}$$

where, for example,

$$|R\Phi_i(R)\rangle = |\,R\rangle|\Phi_i(R)\rangle \tag{3}$$

Inserting resolutions of the identity

$$\int \mathrm{d}R' \sum_{i'} |R'\Phi_{i'}(R')\rangle\langle R'\Phi_{i'}(R')| = \hat{1} \tag{4}$$

between the various operators, we obtain the following expression for the general electronic correlation function

$$\langle \hat{A}\cdot\hat{B}(t)\rangle = \sum_i \sum_{i'} \sum_{j'} \sum_{i''} \sum_{j''} \int \mathrm{d}R \int \mathrm{d}R' \int \mathrm{d}R''\langle R\Phi_i(R)|\hat{\rho}|\,R''\Phi_{j''}(R'')\rangle\langle R''\Phi_{j''}(R'')|\,\hat{A}\,|R''\Phi_{i''}(R'')\rangle\langle R''\Phi_{i''}(R'')|\,\hat{U}^{\dagger}(t)|R'\Phi_{j'}(R')\rangle\langle R'\Phi_{j'}(R')|\,\hat{B}|R'\Phi_{i'}(R')\rangle\langle R'\Phi_{i'}(R')|\,\hat{U}(t)|\,R\Phi_i(R)\rangle \tag{5}$$

where we used the fact that the electronic operators $\hat{A}$ and $\hat{B}$ are assumed to be diagonal in R. This expression can be read as a concatenation of time propagations and evaluations of matrix elements of the given operators. In particular, one needs to compute the transition amplitude for the system to evolve from electronic state i and nuclear coordinate R to state i' and position R' in a time t and that for an evolution in time $-t$ from state j' and coordinate R' to i'' and R''. These amplitudes are sometimes referred to as forward and backward time propagators.[16−20] One also needs the thermal density matrix element between j'' and R'' and i and R, which can be interpreted as a transition amplitude in imaginary time. At this stage, the propagations correspond to the fully coupled quantum motion of the nuclear and electronic system, so that they may, for example, contain nonadiabatic effects. As for the matrix elements of the electronic operators, it is important for future developments to remember that although we have restricted our choice to operators which are diagonal in the nuclear variables they are in general nondiagonal in the electronic basis.

To move toward a computable expression, we proceed in the usual fashion and develop path integral expressions for the propagators and density matrix elements. The thermal density matrix elements, for example, have the following form

$$\langle R\Phi_i(R)|\hat{\rho}|\,R''\Phi_{j''}(R'')\rangle = \frac{1}{Z}\langle R\Phi_i(R)|\,\exp[-\beta\{\hat{P}^2/2M + \hat{H}_{el}(\hat{R})\}]|\,R''\Phi_{j''}(R'')\rangle \tag{6}$$

Dividing β into N slices of size $\epsilon_\beta = \beta/N$ and inserting $N-1$ resolutions of the identity, eq 4, we obtain a discretized path integral form for this density matrix element. We can thus use a high-temperature approximate Trotter form, so the kth slice in this path integral is given by

$$\langle R_{k+1}\Phi_{i_{k+1}}(R_{k+1})|\,\mathrm{e}^{-\epsilon_\beta[\hat{P}^2/2M+\hat{H}_{el}(\hat{R})]}|\,R_k\Phi_{i_k}(R_k)\rangle = \langle R_{k+1}\Phi_{i_{k+1}}(R_{k+1})|\,\mathrm{e}^{-\epsilon_\beta\hat{P}^2/2M}|R_k\Phi_{i_k}(R_k)\rangle\,\mathrm{e}^{-\epsilon_\beta E_{i_k}(R_k)} \tag{7}$$

The evaluation of the nuclear kinetic propagator matrix elements is complicated by the fact that the instantaneous adiabatic basis states depend on nuclear configuration. The effects of this dependence can be appreciated, for example, by a Taylor series expanding the kinetic propagator in the small parameter ϵ_β

$$\exp[-\epsilon_\beta\hat{P}^2/2M] = 1 + \epsilon_\beta\hbar^2\nabla_R^2/2M + \mathcal{O}(\epsilon_\beta{}^2) \tag{8}$$

To lowest order terms in ϵ_β, the matrix elements of the kinetic part of the propagator thus take the following form

$$\langle R_{k+1}\Phi_{i_{k+1}}(R_{k+1})|\ \mathrm{e}^{-\epsilon_\beta \hat{P}^2/2M}|R_k\Phi_{i_k}(R_k)\rangle = \langle R_{k+1}\Phi_{i_{k+1}}(R_{k+1})|R_k\Phi_{i_k}(R_k)\rangle + \frac{\epsilon_\beta\hbar^2}{2M}[2\langle\Phi_{i_{k+1}}(R_{k+1})|\nabla_R|\Phi_{i_k}(R_k)\rangle\langle R_{k+1}|\nabla_R|R_k\rangle + \langle\Phi_{i_{k+1}}(R_{k+1})|\nabla_R^2|\Phi_{i_k}(R_k)\rangle\langle R_{k+1}|R_k\rangle + \langle\Phi_{i_k+1}(R_{k+1})|\Phi_{i_k}(R_k)\rangle\langle R_{k+1}|\nabla_R^2|\ R_k\rangle] + \mathcal{O}(\epsilon_\beta{}^2) \quad (9)$$

The derivatives with respect to the nuclear coordinates in this expression (and the ones which would have arisen had we used a higher order Taylor expansion for the kinetic propagator) are responsible for coupling the different electronic states in the dynamics of the system and are usually referred to as nonadiabatic coupling terms. In the theoretical developments presented here, we will assume that the nuclear derivatives of the adiabatic electronic wave functions are small, and consequently we will drop all terms containing derivative matrix elements between adiabatic states, for example, matrix elements of the form $\langle\Phi_{i_{k+1}}(R_{k+1})|\nabla_R^n|\Phi_{i_k}(R_k)\rangle$, $n = 1, 2, \ldots$. This is the adiabatic approximation to the dynamics of our system. Dropping all of the terms containing such adiabatic state derivatives from eq 11 and summing the remaining series, we obtain the following result

$$\langle R_{k+1}\Phi_{i_{k+1}}(R_{k+1})|\ \mathrm{e}^{-\epsilon_\beta \hat{P}^2/2M}|R_k\Phi_{i_k}(R_k)\rangle_{\mathrm{ad}} = \langle\Phi_{i_{k+1}}(R_{k+1})|\Phi_{i_k}(R_k)\rangle\langle R_{k+1}|\ \mathrm{e}^{-\epsilon_\beta \hat{P}^2/2M}|R_k\rangle \quad (10)$$

This can be further simplified by expanding the adiabatic electronic wave function in $(R_{k+1} - R_k)$, the nuclear displacement between adjacent imaginary time points. Thus, we write the electronic functions in the above brackets as

$$\Phi_{i_{k+1}}(R_{k+1}) = \Phi_{i_{k+1}}(R_k) + \nabla_R\Phi_{i_{k+1}}(R_k)(R_{k+1} - R_k) + \mathcal{O}[(R_{k+1} - R_k)^2] \quad (11)$$

Neglecting all derivatives of the adiabatic states with respect to nuclear variables in this expression, consistent with the adiabatic approximation previously enforced, the high-temperature density matrix elements are

$$\langle R_{k+1}\Phi_{i_{k+1}}(R_{k+1})|\ \mathrm{e}^{-\epsilon_\beta[\hat{P}^2/2M+\hat{\mathrm{H}}_{\mathrm{el}}(\hat{R})]}|R_k\Phi_{i_k}(R_{\mathrm{k}})\rangle_{\mathrm{ad}} = \delta_{i_{k+1}i_k}\left[\int\frac{\mathrm{d}P_k}{2\pi\hbar}\,\mathrm{e}^{i[P_k(R_{k+1}-R_k)/\hbar]}\,\mathrm{e}^{-\epsilon_\beta P_k{}^2/2M}\right]\mathrm{e}^{-\epsilon_\beta E_{i_k}(R_k)} \quad (12)$$

where we have inserted a complete set of nuclear momentum eigenstates to evaluate this result.

The density matrix elements at finite temperature then assume the following discretized path integral form

$$\langle R\Phi_i(R)|\hat{\rho}|R''\Phi_{j''}(R'')\rangle_{\mathrm{ad}} \approx \delta_{ij''}\prod_{k=1}^{N-1}\int \mathrm{d}R_k\ \exp\left[-\sum_{l=0}^{N-1}\left\{\frac{m}{2\hbar^2\epsilon_\beta}(R_{l+1} - R_l)^2 + \epsilon_\beta E_i(R_l)\right\}\right] \quad (13)$$

Here, $R_0 = R''$ and $R_N = R$, and the nuclear momentum integrals have been performed analytically. Similar developments for the propagators in the adiabatic approximation give a total of three Kronecker δs, leaving only two state sums, so the electronic correlation function in this adiabatic limit for the evolution in real and imaginary time becomes

$$\langle\hat{A}\cdot\hat{B}(t)\rangle_{\mathrm{ad}} = \sum_i\sum_{i'}\int\mathrm{d}R\int\mathrm{d}R'\int\mathrm{d}R''\ \langle R\Phi_i(R)|\hat{\rho}|R''\Phi_i(R'')\rangle_{\mathrm{ad}}\langle R''\Phi_i(R'')|\hat{A}|\ R''\Phi_{i'}(R'')\rangle\langle R''\Phi_{i'}(R'')|\hat{U}^\dagger(t)|R'\Phi_{i'}(R')\rangle_{\mathrm{ad}}\langle R'\Phi_{i'}(R')|\ \hat{B}|R'\Phi_i(R')\rangle\langle R'\Phi_i(R')|\hat{U}(t)|R\Phi_i(R)\rangle_{\mathrm{ad}} \quad (14)$$

This expression is completely analogous to eq 5 with the important difference that all propagations are restricted to be adiabatic so that no electronic transitions induced by the dynamics are allowed. Notice that the overall path obtained by combining the propagations in real and imaginary time is closed as it has to be since the correlation function is given by a trace. However, since the electronic operators are in general nondiagonal in the adiabatic basis states, these operator matrix elements connect adiabatic propagation and density matrix path segments on different electronic surfaces, and the expression above therefore still involves more than single state motion.

To appreciate the consequences of this observation and proceed with the development of the approximations leading to our scheme for the calculation of the electronic correlation function, we now generalize the approach presented in recent work by Poulsen and Rossky[7] to the case just described. Thus, we write the adiabatic propagator matrix elements in the following phase space path integral form where we retain the momentum integrals analogous to those in eq 12.

$$\langle R'\Phi_i(R')|\ \hat{U}(t)|\ R\Phi_i(R)\rangle_{\mathrm{ad}} \approx \langle R'|\ \exp[-it\hat{H}_i/\hbar]|R\rangle \approx \prod_{k=1}^{N-1}\int\mathrm{d}R_k\int\frac{\mathrm{d}P_k}{2\pi\hbar}\int\frac{\mathrm{d}P_N}{2\pi\hbar}\exp[iS^N{}_i/\hbar] \quad (15)$$

with

$$S_i^N = \sum_{k=1}^{N}[P_k(R_k - R_{k-1}) - \epsilon_t\{P_k{}^2/2M + E_i(R_k)\}] \quad (16)$$

This propagator involves paths that originate at nuclear configuration $R = R_0$ and evolve adiabatically on electronic surface E_i forward to time t when they arrive at configuration $R' = R_N$. The other propagator appearing in eq 16 starts at the configuration where the forward propagation finished $R' = \tilde{R}_N$ but now evolves backward in time for duration t on the adiabatic electronic surface $E_{i'}$ arriving at configuration $R'' = \tilde{R}_0$. Denoting this backward time path by $(\tilde{R}_k,\tilde{P}_k)$, we have

$$\langle R''\Phi_{i'}(R'')|\ \hat{U}^\dagger(t)|R'\Phi_{i'}(R')\rangle_{\mathrm{ad}} \approx \langle R''|\ \exp[it\hat{H}_{i'}/\hbar]|\ R'\rangle \approx \prod_{k=1}^{N-1}\int\mathrm{d}\tilde{R}_k\int\frac{\mathrm{d}\tilde{P}_k}{2\pi\hbar}\int\frac{\mathrm{d}\tilde{P}_N}{2\pi\hbar}\exp[-i\tilde{S}^N_{i'}/\hbar] \quad (17)$$

where

$$\tilde{S}_{i'}^N = \sum_{k=1}^{N}[\tilde{P}_k(\tilde{R}_k - \tilde{R}_{k-1}) - \epsilon_t\{\tilde{P}_k{}^2/2M + E_{i'}(\tilde{R}_k)\}] \quad (18)$$

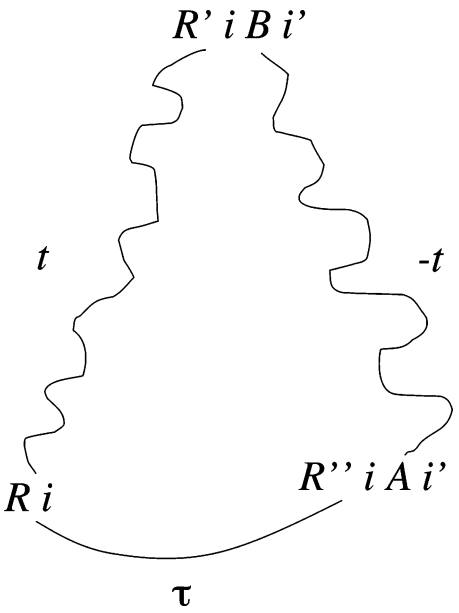

Figure 1. Schematic diagram of relevant paths for adiabatic electronic autocorrelation function calculation.

In Figure 1, we show a schematic diagram of the structure of the paths arising from the adiabatic propagators and density matrix elements that must be integrated over in our electronic correlation function calculation. As mentioned before, because of the presence of the electronic operator matrix element, the forward and backward time adiabatic propagators give paths that evolve in general on different adiabatic potential surfaces. The phases corresponding to these pairs of paths sum up to give the overall phase of a given round-trip path.

The effect of the total phase factor can be better appreciated by changing variables to rewrite the correlation function in terms of mean and difference path variables defined as

$$\bar{R}_k = (R_k + \tilde{R}_k)/2 \quad \text{and} \quad \Delta R_k = R_k - \tilde{R}_k \tag{19}$$

so

$$R_k = \bar{R}_k + \Delta R_k/2 \quad \text{and} \quad \tilde{R}_k = \bar{R}_k - \Delta R_k/2 \tag{20}$$

with similar expressions for the mean and difference momentum path variables.

We begin by substituting these expressions in eq 14, expanding the action difference $S_i - \tilde{S}_{i'}$ coming from the combined forward and backward discrete path integral propagators to linear order in path difference variables, and assuming that the operators of interest have phases that are slowly varying compared to those coming from the propagators. The relevant phase of the integrand in the correlation function thus becomes

$$S_i^N - \tilde{S}_{i'}^N = \sum_{k=1}^{N}\left\{\bar{P}_k(\Delta R_k - \Delta R_{k-1}) + \Delta P_k(\bar{R}_k - \bar{R}_{k-1}) - \epsilon_t\left[\bar{P}_k \Delta P_k/M + [E_i(\bar{R}_k) - E_{i'}(\bar{R}_k)] + \frac{1}{2}[\nabla_R E_i(\bar{R}_k) + \nabla_R E_{i'}(\bar{R}_k)]\Delta R_k\right]\right\} \tag{21}$$

Notice that to obtain this result the adiabatic potentials have also been expanded to linear order in deviations about the mean path.

Following Poulsen and Rossky,[7] we separate out the terms in this sum that contain end point path difference coordinates, ΔR_0 and ΔR_N, common to this propagator product, the density matrix, and operator factors, so we rewrite this integrand phase as

$$S_i^N - \tilde{S}_{i'}^N = \bar{P}_N \Delta R_N - \bar{P}_1 \Delta R_0 - \frac{\epsilon_t}{2}[\nabla_R E_i(\bar{R}_N) + \nabla_R E_{i'}(\bar{R}_N)]\Delta R_N - \epsilon_t \sum_{k=1}^{N-1}\left\{\left(\frac{\bar{P}_{k+1} - \bar{P}_k}{\epsilon_t}\right) + \frac{1}{2}[\nabla_R E_i(\bar{R}_k) + \nabla_R E_{i'}(\bar{R}_k)]\right\}\Delta R_k - \epsilon_t \sum_{k=1}^{N}\left\{\frac{P_k}{M} - \left(\frac{\bar{R}_k - \bar{R}_{k-1}}{\epsilon_t}\right)\right\}\Delta P_k - \epsilon_t \sum_{k=1}^{N}[E_i(\bar{R}_k) - E_{i'}(\bar{R}_k)] \tag{22}$$

Next, we substitute this linearized approximation for the phase of the propagator product into eq 14. Taking into account the path boundary conditions

$$R = R_0 \quad R'' = \tilde{R}_0 \quad R' = R_N = \tilde{R}_N \tag{23}$$

the integrals in eq 16 can be expressed in terms of integrals over sum and difference variables of the end points

$$\bar{R}_0 = \frac{R_0 + \tilde{R}_0}{2} = \frac{R + R''}{2}$$

$$\Delta R_0 = R_0 - \tilde{R}_0 = R - R''$$

$$\bar{R}_N = \frac{R_N + \tilde{R}_N}{2} = R' \tag{24}$$

(note that $\Delta R_N = 0$) to get

$$\langle \hat{A}\cdot\hat{B}(t)\rangle_{\text{ad}}^{\text{lin}} = \sum_i \sum_{i'} \int d\bar{R}_0 \int d\Delta R_0 \int d\bar{R}_N \int \frac{d\bar{P}_N}{2\pi\hbar} \int \frac{d\Delta P_N}{2\pi\hbar} \left(\prod_{k=1}^{N-1} \int d\bar{R}_k \int d\Delta R_k \int \frac{d\bar{P}_k}{2\pi\hbar} \int \frac{d\Delta P_k}{2\pi\hbar}\right) \exp\left[\frac{-i}{\hbar}\bar{P}_1 \Delta R_0\right] \rho_i^{\text{ad}}(\bar{R}_0 + \Delta R_0/2, \bar{R}_0 - \Delta R_0/2; \beta) A_{ii'}(\bar{R}_0 - \Delta R_0/2) B_{i'i}(\bar{R}_N) \exp\left[\frac{-i\epsilon_t}{\hbar}\sum_{k=1}^{N-1}\left\{\left(\frac{\bar{P}_{k+1} - \bar{P}_k}{\epsilon_t}\right) + \frac{1}{2}[\nabla_R E_i(\bar{R}_k) + \nabla_R E_{i'}(\bar{R}_k)]\right\}\Delta R_k\right] \exp\left[\frac{-i\epsilon_t}{\hbar}\sum_{k=1}^{N}\left\{\frac{\bar{P}_k}{M} - \left(\frac{\bar{R}_k - \bar{R}_{k-1}}{\epsilon_t}\right)\right\}\Delta P_k\right] \exp\left[\frac{-i\epsilon_t}{\hbar}\sum_{k=1}^{N}[E_i(\bar{R}_k) - E_{i'}(\bar{R}_k)]\right] \tag{25}$$

In this expression, ρ_i^{ad} is the adiabatic density matrix, eq 13, written in terms of the sum and difference variables. We can interpret the integral over ΔR_0 as the following Wigner transformation

$$[\rho_i^{\mathrm{ad}} A_{ii'}]_{\mathrm{W}}(\bar{R}_0, \bar{P}_1) = \int \mathrm{d}\Delta R_0\, \mathrm{e}^{-i\bar{P}_1\Delta R_0/\hbar} \rho_i^{\mathrm{ad}}(\bar{R}_0 + \Delta R_0/2, \bar{R}_0 - \Delta R_0/2;\beta) A_{ii'}(\bar{R}_0 - \Delta R_0/2) \quad (26)$$

To evaluate this quantity, we first approximate the adiabatic density matrix elements by the high-temperature limit using $N = 1$ and write the result in terms of the sum and difference coordinates $\bar{R}_0$ and ΔR_0, thus

$$\rho_i^{\mathrm{ad}}(\bar{R}_0 + \Delta R_0/2, \bar{R}_0 - \Delta R_0/2;\beta) = \exp\left[-\frac{M}{2\hbar^2\beta}(\Delta R_0)^2 - \beta E_i(\bar{R}_0 - \Delta R_0/2)\right] \quad (27)$$

We further assume that the electronic matrix element $A_{ii'}$ and the $\exp[-\beta E_i]$ factor are slowly varying functions of nuclear coordinates compared to the Gaussian in the difference variable and evaluate the integral over ΔR_0 to obtain

$$[\rho_i^{\mathrm{ad}} A_{ii'}]_{\mathrm{W}}(\bar{R}_0, \bar{P}_1) \approx \left(\frac{2\pi\hbar^2\beta}{m}\right)^{3N/2} \exp[-\beta E_i(\bar{R}_0)] \exp[-\beta \bar{P}_1^2/2M] A_{ii'}(\bar{R}_0) \quad (28)$$

Substituting this approximation for the density matrix into the expression for the correlation function, we obtain

$$\begin{aligned}\langle \hat{A}\cdot\hat{B}(t)\rangle_{\mathrm{ad}}^{\mathrm{lin}} \approx \sum_i \sum_{i'} \int \mathrm{d}\bar{R}_0 \int \mathrm{d}\bar{P}_1 \exp[-\beta\{\bar{P}_1^2/2M + E_i(\bar{R}_0)\}] A_{ii'}(\bar{R}_0) \int \mathrm{d}\bar{R}_1 \int \frac{\mathrm{d}\Delta P_1}{2\pi\hbar} \exp\left[\frac{-i\epsilon_t}{\hbar}\left\{\frac{\bar{P}_1}{M} - \left(\frac{\bar{R}_1 - \bar{R}_0}{\epsilon_t}\right)\right\}\Delta P_1\right] \exp\left[\frac{-i\epsilon_t}{\hbar}[E_i(\bar{R}_1) - E_{i'}(\bar{R}_1)]\right] \int \frac{\mathrm{d}\bar{P}_2}{2\pi\hbar} \int \mathrm{d}\Delta R_1 \exp\left[\frac{-i\epsilon_t}{\hbar}\left\{\left(\frac{\bar{P}_2 - \bar{P}_1}{\epsilon_t}\right) + \frac{1}{2}[\nabla_R E_i(\bar{R}_1) + \nabla_R E_{i'}(\bar{R}_1)]\right\}\Delta R_1\right] \int \mathrm{d}\bar{R}_2 \int \frac{\mathrm{d}\Delta P_2}{2\pi\hbar} \exp\left[\frac{-i\epsilon_t}{\hbar}\left\{\frac{\bar{P}_2}{M} - \left(\frac{\bar{R}_2 - \bar{R}_1}{\epsilon_t}\right)\right\}\Delta P_2\right] \exp\left[\frac{-i\epsilon_t}{\hbar}[E_i(\bar{R}_2) - E_{i'}(\bar{R}_2)]\right] \int \frac{\mathrm{d}\bar{P}_3}{2\pi\hbar} \int \mathrm{d}\Delta R_2 \exp\left[\frac{-i\epsilon_t}{\hbar}\left\{\left(\frac{\bar{P}_3 - \bar{P}_2}{\epsilon_t}\right) + \frac{1}{2}[\nabla_R E_i(\bar{R}_2) + \nabla_R E_{i'}(\bar{R}_2)]\right\}\Delta R_2\right] \cdots \int \frac{\mathrm{d}\bar{P}_N}{2\pi\hbar} \int \mathrm{d}\Delta R_{N-1} \exp\left[\frac{-i\epsilon_t}{\hbar}\left\{\left(\frac{\bar{P}_N - \bar{P}_{N-1}}{\epsilon_t}\right) + \frac{1}{2}[\nabla_R E_i(\bar{R}_{N-1}) + \nabla_R E_{i'}(\bar{R}_{N-1})]\right\}\Delta R_{N-1}\right] \int \mathrm{d}\bar{R}_N \int \frac{\mathrm{d}\Delta P_N}{2\pi\hbar} \exp\left[\frac{-i\epsilon_t}{\hbar}\left\{\frac{\bar{P}_N}{M}\left(\frac{\bar{R}_N - \bar{R}_{N-1}}{\epsilon_t}\right)\right\}\Delta P_N\right] \exp\left[\frac{-i\epsilon_t}{\hbar}[E_i(\bar{R}_N) - E_{i'}(\bar{R}_N)]\right] B_{i'i}(\bar{R}_N) \quad (29)\end{aligned}$$

The integrals over the path difference variables can now be performed analytically since $\int \mathrm{d}k \exp[ikf(x)] = 2\pi\delta(f(x))$ giving

$$\begin{aligned}\langle \hat{A}\cdot\hat{B}(t)\rangle_{\mathrm{ad}}^{\mathrm{lin}} \approx \sum_i \sum_{i'} \int \mathrm{d}\bar{R}_0 \int \mathrm{d}\bar{P}_1 \exp[-\beta\{\bar{P}_1{}^2/2M + E_i(\bar{R}_0)\}] A_{ii'}(\bar{R}_0) \int \mathrm{d}\bar{R}_1\, \delta\left(\frac{\bar{P}_1}{M} - \left(\frac{\bar{R}_1 - \bar{R}_0}{\epsilon_t}\right)\right) \exp\left[\frac{-i\epsilon_t}{\hbar}[E_i(\bar{R}_1) - E_{i'}(\bar{R}_1)]\right] \int \mathrm{d}\bar{P}_2\, \delta\left(\left(\frac{\bar{P}_2 - \bar{P}_1}{\epsilon_t}\right) + \frac{1}{2}[\nabla_R E_i(\bar{R}_1) + \nabla_R E_{i'}(\bar{R}_1)]\right) \int \mathrm{d}\bar{R}_2\, \delta\left(\frac{\bar{P}_2}{M} - \left(\frac{\bar{R}_2 - \bar{R}_1}{\epsilon_t}\right)\right) \exp\left[\frac{-i\epsilon_t}{\hbar}[E_i(\bar{R}_2) - E_{i'}(\bar{R}_2)]\right] \int \mathrm{d}\bar{P}_3\, \delta\left(\left(\frac{\bar{P}_3 - \bar{P}_2}{\epsilon_t}\right) + \frac{1}{2}[\nabla_R E_i(\bar{R}_2) + \nabla_R E_{i'}(\bar{R}_2)]\right) \cdots \int \mathrm{d}\bar{P}_N\, \delta\left(\left(\frac{\bar{P}_N - \bar{P}_{N-1}}{\epsilon_t}\right) + \frac{1}{2}[\nabla_R E_i(\bar{R}_{N-1}) + \nabla_R E_{i'}(\bar{R}_{N-1})]\right) \int \mathrm{d}\bar{R}_N\, \delta\left(\frac{\bar{P}_N}{M} - \left(\frac{\bar{R}_N - \bar{R}_{N-1}}{\epsilon_t}\right)\right) \exp\left[\frac{-i\epsilon_t}{\hbar}[E_i(\bar{R}_N) - E_{i'}(\bar{R}_N)]\right] B_{i'i}(\bar{R}_N) \quad (30)\end{aligned}$$

This result is readily interpreted in terms of an interated time stepping integration of classical-like equations of motion for the mean path. Thus, we sample an initial phase space point $(\bar{R}_0, \bar{P}_1)$ from a Gibbs distribution for adiabatic electronic potential surface i and compute the electronic matrix element at this configuration $A_{ii'}(\bar{R}_0)$. Next, we use the first δ function to perform the integration over $\bar{R}_1$, which results in a simple algebraic equation for this new configuration in terms of the initial conditions. Proceeding, we evaluate the electronic potential difference at this point and accumulate the relevant phase factor for the advancing trajectory. We complete the step by computing the average force from the two electronic potentials i and i' and perform the integral over $\bar{P}_2$, which determines this new momentum in terms of the previous momentum and mean force. We iterate this process until $\bar{R}_N$ where we evaluate the final electronic matrix element $B_{i'i}(\bar{R}_N)$.

In summary, the approximate high-temperature, linearized, adiabatic electronic time correlation function can be computed from the following expression

$$\begin{aligned}\langle \hat{A}\cdot\hat{B}(t)\rangle_{\mathrm{ad}}^{\mathrm{lin}} \approx \sum_i \sum_{i'} \int \mathrm{d}\bar{R}_{ii'}(0) \int \mathrm{d}\bar{P}_{ii'}(0)\, \mathrm{e}^{-\beta\{\bar{P}_{ii'}{}^2(0)/2M + E_i(\bar{R}_{ii'}(0))\}} A_{ii'}(\bar{R}_{ii'}(0)) B_{i'i}(\bar{R}_{ii'}(t))\, \mathrm{e}^{-i/\hbar \int_0^t \mathrm{d}t'\{E_i(\bar{R}_{ii'}(t')) - E_{i'}(\bar{R}_{ii'}(t'))\}} \quad (31)\end{aligned}$$

where we redefined the initial conditions as

$$\bar{R}_0 = \bar{R}_{ii'}(0) \quad \text{and} \quad \bar{P}_1 = \bar{P}_{ii'}(0) \quad (32)$$

and $\bar{R}_{ii'}(t')$ represents the coordinate of the system at time t' along a classical trajectory that evolves according to

$$M\frac{\mathrm{d}\bar{R}_{ii'}}{\mathrm{d}t}(t) = \bar{P}_{ii'}(t) \quad (33)$$

and

$$\frac{\mathrm{d}\bar{P}_{ii'}}{\mathrm{d}t}(t) = -\frac{1}{2}[\nabla_R E_i(\bar{R}_{ii'}(t)) + \nabla_R E_{i'}(\bar{R}_{ii'}(t))] \quad (34)$$

Notice that if we are considering the contribution to the sum in eq 31 given by an off-diagonal element of the electronic operators (i.e., $i \neq i'$), then the classical equations of motion written above describe an (adiabatic) evolution governed by a

potential determined by the mean of the eigenvalues with indexes i and i'.

The result presented in eq 31 applies for arbitrary operators at all times. If however one is interested in the long time limit of a correlation function, as is generally the case for transport coefficients,[21] then the result simplifies considerably. A stationary phase analysis can be performed to obtain the general result in this limit

$$\lim_{t\to\infty}\langle\hat{A}\hat{B}(t)\rangle_{\mathrm{ad}}^{\mathrm{lin}} \approx \sum_i \int \mathrm{d}\bar{R}_{ii}(0) \int \mathrm{d}\bar{P}_{ii}(0) \, \mathrm{e}^{-\beta\{\bar{P}_{ii}^2(0)/2M + E_i(\bar{R}_{ii}(0))\}} A_{ii}(\bar{R}_{ii}(0)) B_{ii}(\bar{R}_{ii}(t)) \quad (35)$$

The absence of oscillatory phase factors in this expression makes calculations in this limit very efficient. In Appendix A, we show in detail how this result can be obtained in the case of the mean square displacement estimator for diffusion. We also show that by introducing the additional hypothesis that only the ground state is thermally occupied yields a well-known approximation for estimating electronic diffusion coefficients.[14]

In the next section, we will explore how the approximate linearized adiabatic equilibrium time correlation function formalism developed here can be applied to calculate specific dynamical quantities such as the diffusion coefficient of an excess electron in a metal−molten salt solution.

3. Results

The behavior of an excess electron in dilute metal−molten salt solutions has been the subject of many experimental and theoretical studies.[14,15,22,23] The details of the model we employ are exactly the same as the vintage calculations of Selloni and co-workers.[14,23] Specifically, our simulations have been performed on a periodically repeated system of 32 K^+ cations, 31 Cl^- anions, and 1 electron. The mass density was set to $\rho = 1.52 \times 10^3$ kg/m^3 and the temperature to $T = 1300$ K. Selloni and co-workers computed the diffusion constant of the excess electron under these conditions in an adiabatic approximation and obtained results in fair agreement with experiment. They also estimated the absorption line shape of the excess electron in the Franck−Condon approximation. Below, we compare their results and experimental observations with calculations based on our new theory. We also report results at a higher temperature $T = 1800$ K to investigate the effects of increasing the nuclear kinetic energy on the adiabatic hypothesis and on diffusion. To address the first point, we monitor the evolution of the adiabatic expansion coefficients along a characteristic adiabatic ground state nuclear trajectory using the procedure outlined in Appendix B.

Our analysis at $T = 1300$ K shows negligible departure from pure adiabatic evolution with excited state expansion coefficients on the order of 10^{-5} throughout. However, trajectories at $T = 1800$ K show more pronounced nonadiabatic effects. For example, in Figure 2 we see that the ground state amplitude drops by on the order of 10% in various localized "transition" regions. Comparison with the electronic state energies, also displayed in this figure, reveals that these events occur at avoided crossings where large displacements of the electron take place as shown in the bottom panel. (Note that the displacement presented in this figure was computed with the periodic estimator defined in eq 44.[24]) Despite this increased nonadiabatic activity at higher temperatures, in the following we present results for the adiabatic approach described in this paper. The generalization to include nonadiabatic dynamics in correlation function calculations is the subject of much on going research.[25,26]

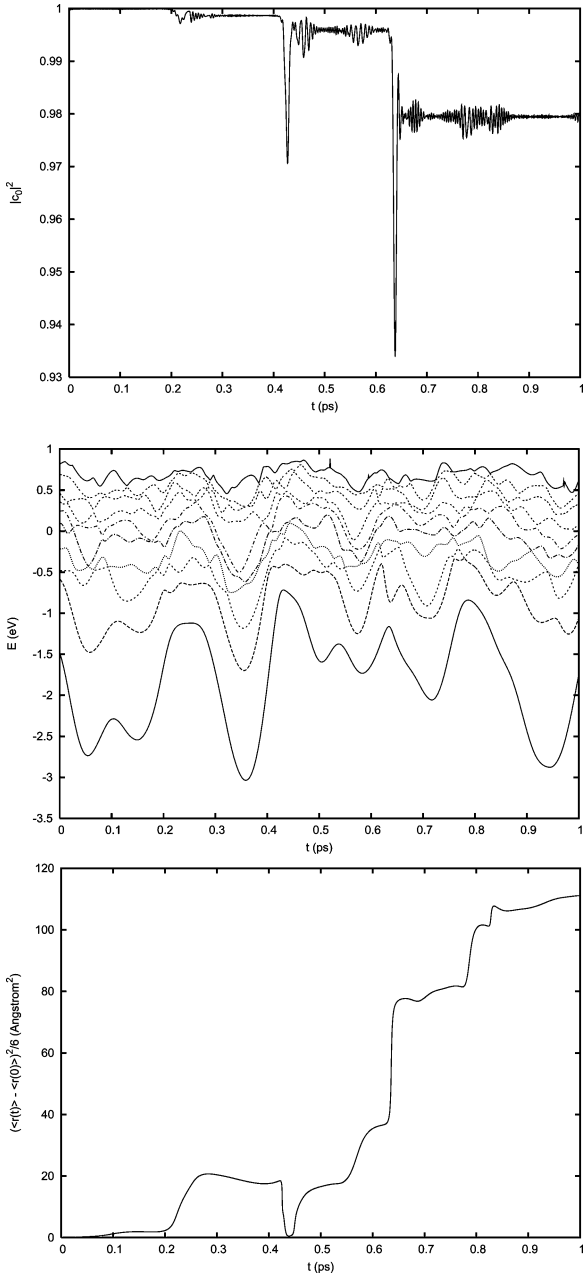

Figure 2. Evolution of $|c_0|^2$ (upper panel) and the lowest nine eigenvalues (middle panel) along a 1 ps trajectory at $T = 1800$ K. The lower panel shows the electron's mean square displacement along the same trajectory.

To obtain the diffusion constant, D, we consider two alternative equilibrium time correlation function approaches. First, D can be obtained from the long time limit of the slope of the time-dependent mean square displacement of the electron from its starting position. The quantum expression for this estimator is

$$D = \frac{1}{6}\lim_{t\to\infty}\frac{\mathrm{d}}{\mathrm{d}t}\langle(\hat{\boldsymbol{r}}(0) - \hat{\boldsymbol{r}}(t))^2\rangle \quad (36)$$

This average is not of the form discussed in the previous section, but it can be cast as such via the following observation. The straightforward implementation of this position-based estimator for the diffusion poses problems for a periodic system.[24] In our simulations, we will represent the system of interest using the periodic repetition of a cubic box of length L. We therefore use a periodic estimator chosen as

$$D_l^P(t) = \lim_{k\to 0} \frac{1}{2} k^2 \langle \hat{R}_l(k,t) \hat{R}_l^*(k,t) \rangle \tag{37}$$

where

$$\hat{R}_l(k,t) = (e^{ik\hat{r}_l(t)} - e^{ik\hat{r}_l(0)}) \tag{38}$$

with $\hat{r}_l$ being the lth component of the electron position operator, and the possible wave-vector components are $k = 2m\pi/L$ (m nonzero integer).

The right-hand side of eq 37 can be written in the form of a sum of correlation functions of the type discussed in the previous section by expanding the above product. For example, for the lth component, one obtains

$$D_l^P(t) = \lim_{k\to 0} D_l^P(k,t) \equiv \lim_{k\to 0} \frac{1}{2k^2} (2 - \langle e^{ik\hat{r}_l(0)}\, e^{-ik\hat{r}_l(t)} + e^{ik\hat{r}_l(t)}\, e^{-ik\hat{r}_l(0)} \rangle) \tag{39}$$

Our estimator is related to eq 36 by

$$D = \frac{1}{3} \lim_{t\to\infty} \frac{d}{dt} \sum_l D_l^P(t) \tag{40}$$

The calculations reported below have been performed with finite values of k; therefore the numerical estimator we use is

$$D(k) = \frac{1}{3} \lim_{t\to\infty} \frac{d}{dt} \sum_l D_l^P(k,t) \tag{41}$$

and extrapolate to $k \to 0$.

In Figure 3, we show the behavior of the first few terms of

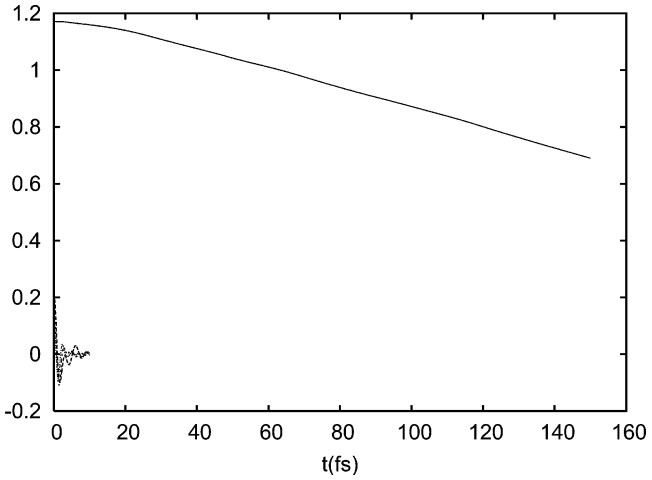

Figure 3. Contributions from diagonal (0,0) (solid curve) and off-diagonal ((0,1), (0,2), (0,3)) (various dashed curves) matrix elements to $\langle e^{ik\hat{r}_l(0)}\, e^{-ik\hat{r}_l(t)} + e^{ik\hat{r}_l(t)}\, e^{-ik\hat{r}_l(0)} \rangle$. The results shown here are for $\hat{r}_l = \hat{x}$; very similar behavior is observed for other components

the sum over pairs of states in eq 31 for $\langle e^{ik\hat{r}_l(0)}\, e^{-ik\hat{r}_l(t)} + e^{ik\hat{r}_l(t)}\, e^{-ik\hat{r}_l(0)} \rangle$. In evaluating the double sum in the correlation function, we restrict the starting state to be $|\Phi_0\rangle$ ($i = 0$ in eq 31) as this is the only state with appreciable thermal population at the temperatures of our simulations. As can be seen from the figure, the diagonal term (corresponding to $(i,i') = (0,0)$ in eq 31) dominates throughout while the off-diagonal terms (corresponding to $(i,i') = (0,n)$ $\forall$ integer $n > 0$ in eq 31) rapidly decay to zero. It is also interesting to note that the zero time value of the correlation function obtained by summing the first four terms is 1.8, within 20% of the analytic value of 2.0, indicating rapid convergence with number of states.

Since the smallest value of k that can be obtained with a given simulation box length is $k = 2\pi/L$, achieving the limit of a small wave vector in eq 37 with a computationally feasible box length is problematic. For example, varying the k over values $6\pi/L$, $4\pi/L$, and $2\pi/L$ gives diffusion constant estimates of $D(k) = 1 \times 10^{-5}$, 1×10^{-4}, and 8×10^{-4} cm^2 s^{-1} respectively. Although this sequence of values is approaching the experimental result of $D_{exp} = 3 \times 10^{-3}$ cm^2 s^{-1}, the minimum k compatible with the box length used in our simulations is still too large for reliable extrapolation.

However, as mentioned in the previous section, in Appendix A we show that the long time behavior of the periodic estimator can be obtained from only diagonal ground state contributions to the double sum in eq 31. The result we find is

$$D_{ad} = \frac{1}{6} \lim_{t\to\infty} \frac{d}{dt} \int dR(0) \int dP(0)\, e^{-\beta\{P^2(0)/2M + E_0(R(0))\}} (\langle r \rangle_{\Phi_0(R(0))} - \langle r \rangle_{\Phi_0(R(t))})^2 / Z_0 \tag{42}$$

where $\langle r \rangle_{\Phi_0(R(t))} = \langle \Phi_0(R(t)) | \hat{r} | \Phi_0(R(t)) \rangle$ and

$$Z_0 = \int dR(0) \int dP(0)\, e^{-\beta\{P^2(0)/2M + E_0(R(0))\}} \tag{43}$$

The estimator defined in eq 42 was used by Selloni et al.[14] together with the periodic expectation value defined by Resta[24]

$$\langle \hat{r} \rangle = \frac{L}{2\pi} \mathrm{Im}[\ln \langle \Phi_0 |\, e^{i2\pi/L\hat{r}} | \Phi_0 \rangle] \tag{44}$$

in their calculations yielding a value of $D_S = 2 \times 10^{-3}$ cm^2 s^{-1}. The convergence of this approach with box length is superior to the more general estimator described above. Resta's formulation, which focuses on expectation values, is not easily generalized to consider the off-diagonal matrix elements required in the most general version of our theory. Both the numerical findings presented in Figure 3 and our stationary phase analysis, however, support the reliability of restricting these calculations to only ground state contributions. We have therefore used this approximation to compute the diffusion constant at both $T = 1300$ K and $T = 1800$ K as a consistency check of our more general approach. The averages of the mean square displacement over ~300 nuclear trajectories at the two temperatures are shown in Figure 5. The long time limiting value of the slope of the curve in the upper panel gives $D_{1300}^{msd} = (1.1 \pm 0.5) \times 10^{-3}$ cm^2 s^{-1} for the run at $T = 1300$ K. This result is somewhat smaller than that reported by Selloni and co-workers. The discrepancy is probably due to the statistical uncertainty in these calculations. A direct comparison is complicated by the absence of error bars in the results of Selloni et al. Our result for the higher-temperature diffusion constant is $D_{1800}^{msd} = (1.9 \pm 0.5) \times 10^{-3}$ cm^2 s^{-1}.

In Figure 4, calculated values of the diffusion constant are compared with experiments. The reasonable agreement between results from approximate mean square displacement calculations (both ours and Selloni's) and the extrapolation of results from our periodic estimator is the first validation of our approach.

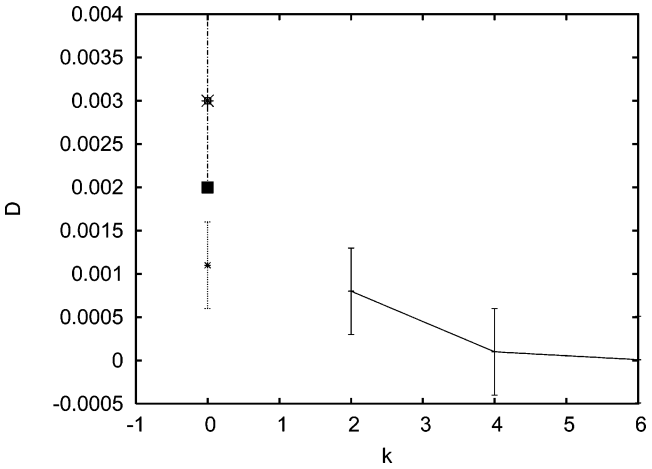

Figure 4. Values of D in cm^2 s^{-1} at $T = 1300$ K obtained with various methods. Periodic position-based estimator is shown for different values of k (in units of π/L) (solid line with crosses). Mean square displacement result using eq 42 (dotted with small asterisk). Diffusion constant from integral of velocity autocorrelation function (dash dot with small square). Results from Selloni et al. (large filled box) and experiment (large asterisk) are also shown.

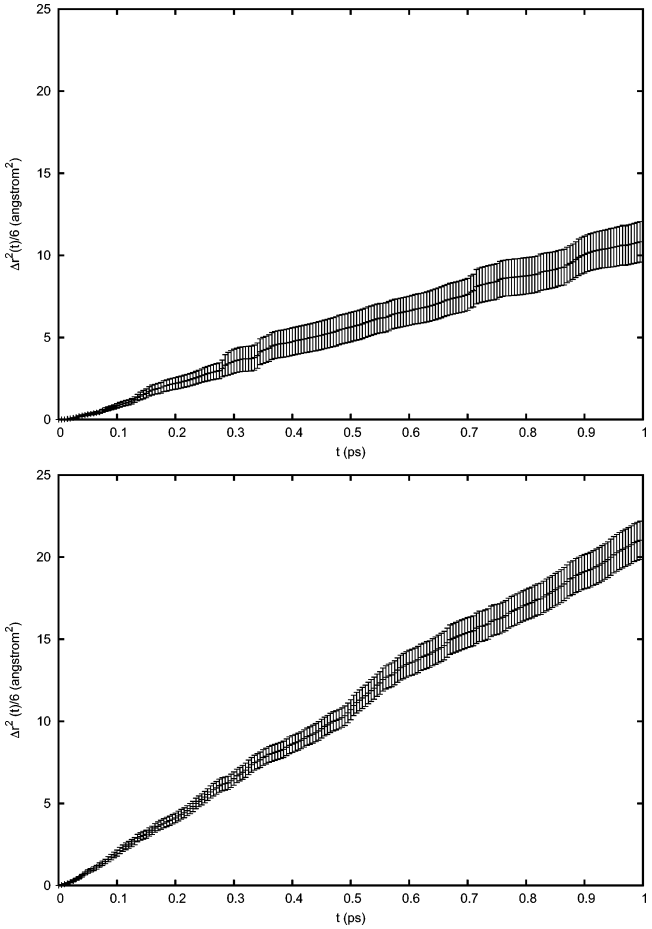

Figure 5. Ground state mean square displacement estimator for excess electron diffusion at $T = 1300$ K (upper panel) and $T = 1800$ K (lower panel).

The second approach we use to estimate D employs the following expression

$$D_v = \frac{1}{3}\int_0^\infty C_{vv}(t)\,\mathrm{d}t \tag{45}$$

where

$$C_{vv}(t) = \langle \hat{v}\hat{v}(t)\rangle = \mathrm{Tr}\{\hat{\rho}\hat{v}\hat{v}(t)\} \tag{46}$$

is the velocity autocorrelation function. The diffusion coefficient computed in this way corresponds to the zero frequency limit of the complex mobility as defined by Kubo.[27]

In Figures 6 and 7, we present the real and imaginary parts of our velocity autocorrelation functions calculated using eq 31

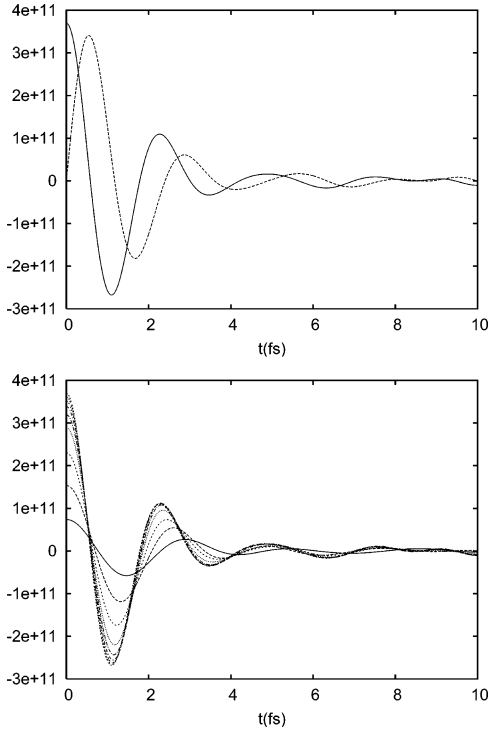

Figure 6. Real (solid) and imaginary (dashed) parts of the velocity autocorrelation at $T = 1300$ K (upper panel). Cumulative contributions to the real part of the velocity autocorrelation function obtained from eq 31 by restricting $i = 0$ and truncating the sum over i' at some maximum value i'_{max}, for $i'_{max} = 1, ..., 9$ (lower panel). Here, the y-axis units are m^2 s^{-2}.

at $T = 1300$ K and $T = 1800$ K, respectively. The diagonal velocity matrix elements in the instantaneous adiabatic electronic basis set are rigorously zero, so the only finite contributions to our estimator come from off-diagonal terms. From eq 31, these contributions are computed using trajectories moving over the mean of the adiabatic potential surfaces associated with the two different states involved in the nonzero off-diagonal velocity matrix elements. In addition, eq 33 indicates that each of these off-diagonal contributions must be weighted by a phase factor that oscillates in time at a frequency determined by the energy gap between this pair of different states. These phase-weighted contributions must be added for each pair of different adiabatic states included in our representation since precise details of both the short and the long time history of the velocity autocorrelation function are necessary if its integral is to be computed accurately.

In the figures, we demonstrate the convergence of these correlation functions with the number of states included by plotting the cumulative contributions to the real part from various off-diagonal terms in the expression for the velocity autocorrelation function. Just as for the position-based estimators, we include only contributions from the ground state in the thermal average. Tests of the completeness of our adiabatic basis in which we compare the mean square velocity at zero time computed directly and summing off-diagonal velocity matrix

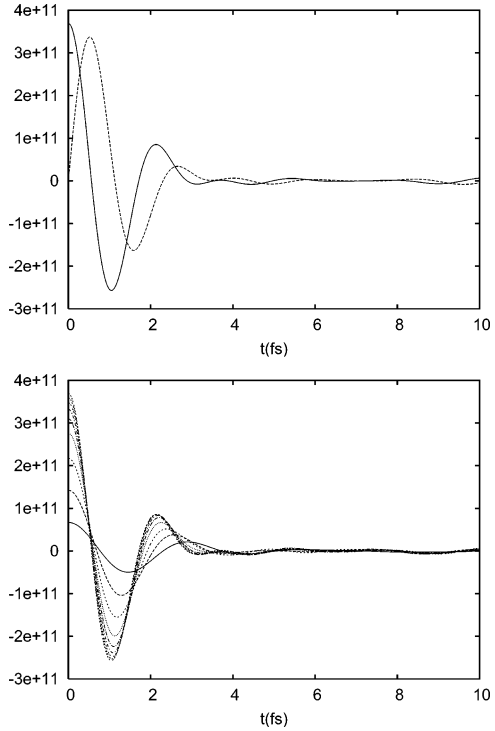

Figure 7. Real (solid) and imaginary (dashed) parts of the velocity autocorrelation at $T = 1800$ K (upper panel). Cumulative contributions to the real part of the velocity autocorrelation function obtained from eq 31 by restricting $i = 0$ and truncating the sum over i' at some maximum value i'_{max}, for $i'_{max} = 1, ..., 9$ (lower panel). Here, the *y*-axis units are $m^2\ s^{-2}$.

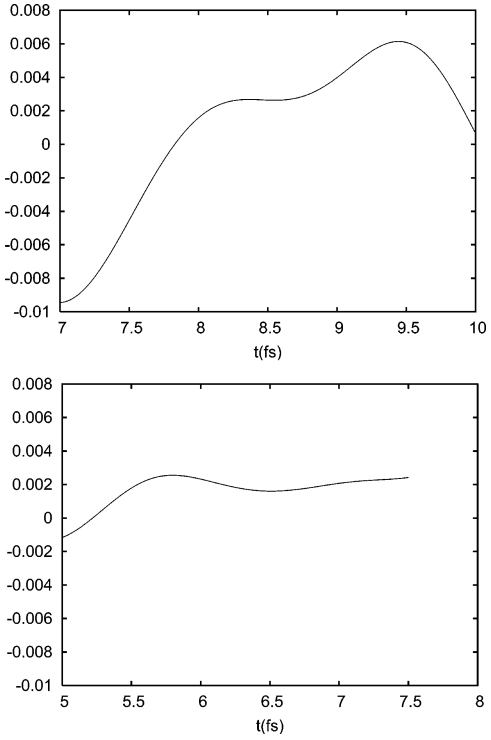

Figure 8. Cumulative time integral of velocity autocorrelation function at $T = 1300$ K (upper panel) and $T = 1800$ K (lower panel). Here the *y*-axis units are $cm^2\ s^{-1}$.

elements (i.e., $\langle\Phi_0|\hat{v}_l^2|\Phi_0\rangle = \Sigma_n^{n_{max}} \langle\Phi_0|\hat{v}_l|\Phi_n\rangle\langle\Phi_n|\hat{v}_l|\Phi_0\rangle$, with $l = x$, y, or z) show that the nine states included in these studies satisfy the completeness relation within ~25%. As we see from the figures, the caging dynamics apparent in the early time oscillations of the averaged correlation function is dominated by the first four terms. At longer times, all state contributions become comparable, and their oscillatory nature makes a reliable representation of the decay of the averaged correlation function problematic. This situation can be contrasted with the behavior of the position-based estimators described above where just the ground state dominates at all times.

In Figure 8, we display the integral of the velocity autocorrelation function versus the upper limit of the time integration in eq 45 to explore the convergence of the diffusion constants obtained from this estimator with respect to this parameter. The situation is clearly very different for the two temperatures. At the lower temperature, coherent oscillations in the correlation function (apparently arising predominantly from the lower state contributions) persist at longer times, thus complicating the estimate of the diffusion coefficient. At $T = 1300$ K, this estimator gives a value of $(3 \pm 2) \times 10^{-3}\ cm^2\ s^{-1}$, the large error bar reflecting the difficulties mentioned above. At higher temperature, the figure shows oscillations around a plateau value, indicating that the decay of the velocity autocorrelation function is sufficiently rapid and that the interference effects among the different terms in the sum are captured reliably. Our estimate for the diffusion coefficient under these conditions is $(2 \pm 0.5) \times 10^{-3}\ cm^2\ s^{-1}$, in good agreement with the position-based estimators discussed above. This agreement confirms that our approximation for the correlation function is accurate enough to preserve the Green−Kubo relation between the mean square displacement and the velocity autocorrelation function expressions for D.

The velocity autocorrelation function can be exploited to calculate the absorption line shape (i.e., the power spectrum of the dipole autocorrelation) as follows

$$I(\omega) = \frac{1}{2\pi\omega^2} \int_{-\infty}^{\infty} C_{vv}(t)\, e^{-i\omega t}\, dt \qquad (47)$$

In Figure 9, we compare the absorption line shape computed using our approach with the result obtained by Selloni et al. using the Franck−Condon approximation and experiment. At 1300 K (upper panel), the peaks of the calculated line shapes coincide and are about 0.3 eV higher in energy than the experimental band.[15] The line width from our calculations agrees very well with experiment, but the Franck−Condon band is significantly narrower. This may be due to inadequate description of the long time behavior of the correlation function in the Franck−Condon approximation, affecting the low-energy tail of the line shape. At higher temperatures, our calculations show (Figure 9, lower panel) a slight red shift and broadening of the line shape consistent with narrowing of the energy gaps.

4. Conclusions

In this paper, we presented a new approach for calculating quantum time correlation functions. Our result generalizes the linearization procedure[7] to the case when electronic operators are measured in the approximation of adiabatic nuclear dynamics. We applied our method to the evaluation of the diffusion coefficient of an excess electron in a metal−molten salt solution and showed that it produces results that are in reasonable agreement with previous calculations and experiments. Furthermore, the theory presented here allows us to understand the nature of the approximations contained in these previous studies and provides a systematic way to improve the heuristic definition of some of the estimators that have been used. With the proposed method, different estimators related by the Green−Kubo formula for diffusion are numerically consistent.

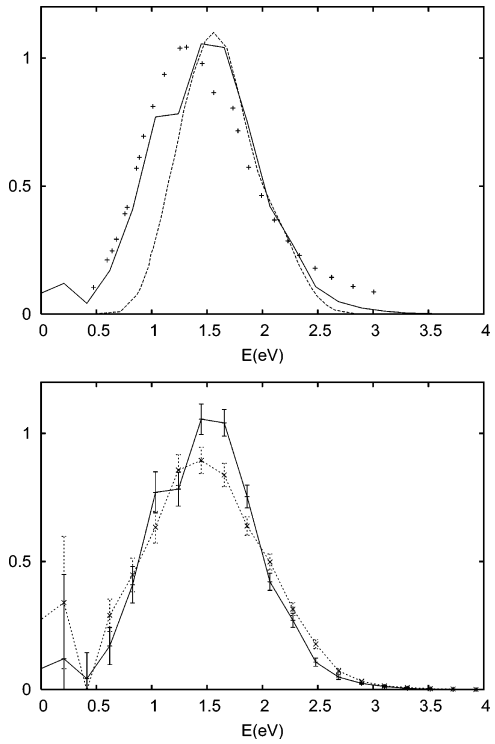

Figure 9. Comparison of spectral line shapes. Upper panel shows results from present calculation (solid curve), calculations performed within the Franck−Condon approximation from ref 14 (dashed curve) (both calculations are at $T = 1300$ K), and experimental results at $T = 1133$ K[15] (crosses). The lower panel compares line shapes from present calculations at $T = 1300$ K (solid curve) and $T = 1800$ K (dotted curve). Error bars grow at lower energies reflecting the larger statistical uncertainties in the longer time correlation function values.

Acknowledgment. We wish to acknowledge useful discussions with T. Castonguay. Financial support from the National Science Foundation (Grant No. CHE-0316856) and the American Chemical Society (Grant No. 39180-AC6) is gratefully acknowledged. D.F.C. wishes to acknowledge the kind hospitality of G.C. and the Dipartimento di Fisica, Università "La Sapienza", and the financial support from the INFM that enabled his Sabbatical visit to Rome. The simulations were carried out mainly on the IBM cluster at the Forschungszentrum Jülich and in part on the IBM cluster at CINECA. Financial support from the INFM grant "Progetto di Calcolo Parallelo" is also acknowledged.

Appendix A. Stationary Phase Analysis of the Position-Based Estimator for the Electronic Diffusion

The calculation of the diffusion coefficient based on the mean square displacement or position autocorrelation function estimator can be considerably simplified since only the asymptotic long time limit of the slope is required.

Imagine evaluating the integrals over initial mean position and momentum $\int d\bar{R}_{ii'}(0) \int d\bar{P}_{ii'}(0)$ in eq 31 by stationary phase for each correlation function of the form $\langle e^{ik\hat{r}_l(0)} e^{-ik\hat{r}_l(t)} + e^{ik\hat{r}_l(t)} e^{-ik\hat{r}_l(0)}\rangle$ necessary to evaluate the periodic estimator described in section 3. The phase of the integrand in eq 31

$$\phi(\bar{R}_{ii'}(0), \bar{P}_{ii'}(0)) = \int_0^t dt' \{E_i(\bar{R}_{ii'}(t')) - E_{i'}(\bar{R}_{ii'}(t'))\} \quad (48)$$

is stationary with respect to variations in the initial conditions $\delta\bar{R}_{ii'}(0)$ and $\delta\bar{P}_{ii'}(0)$ if

$$\delta\phi = \frac{\partial\phi}{\partial\bar{R}_{ii'}(0)} \delta\bar{R}_{ii'}(0) + \frac{\partial\phi}{\partial\bar{P}_{ii'}(0)} \delta\bar{P}_{ii'}(0) = 0 \quad (49)$$

This condition requires

$$\int dt' \left(\frac{\partial E_i}{\partial\bar{R}_{ii'}(t')} - \frac{\partial E_{i'}}{\partial\bar{R}_{ii'}(t')}\right)\left(\frac{\partial\bar{R}_{ii'}(t')}{\partial\bar{R}_{ii'}(0)} \delta\bar{R}_{ii'}(0) + \frac{\partial\bar{R}_{ii'}(t')}{\partial\bar{P}_{ii'}(0)} \delta\bar{P}_{ii'}(0)\right) = 0 \quad (50)$$

for arbitrary variations $\delta\bar{R}_{ii'}(0)$ and $\delta\bar{P}_{ii'}(0)$. At long times, nuclear motion in the condensed phase systems of interest becomes chaotic, so the monodromy derivative factors in the above expression, which gauge trajectory end point stability with respect to variation in trajectory initial conditions, diverge. The stationary phase condition can be satisfied if the forces from the two electronic surfaces are always the same which, in general, implies that $i = i'$. The long time stationary phase condition thus gives a Kronecker $\delta_{ii'}$ that kills one of the sums in eq 31, reducing it to a Boltzmann weighted sum over classical trajectories moving on adiabatic potentials and only diagonal elements of the electronic operators so that, for example,

$$\lim_{t\to\infty} \langle e^{ik\hat{r}_l(0)} e^{-ik\hat{r}_l(t)}\rangle_{ad}^{lin} = \frac{1}{Z}\sum_i \int dR_i(0) \int dP_i(0) \, e^{-\beta\{P_i^2(0)/2M + E_i(R_i(0))\}} e_{ii}^{ikr_l}(R_i(0)) \, e_{ii}^{ikr_l}(R_i(t)) \quad (51)$$

where

$$Z = \sum_i \int dR_i(0) \int dP_i(0) \, e^{-\beta\{P_i^2(0)/2M + E_i(R_i(0))\}} \quad (52)$$

and

$$e_{ii}^{ikr_l}(R_i(0)) = \langle\Phi_i(R_i(0))| \, e^{ik\hat{r}_l}|\Phi_i(R_i(0))\rangle \quad (53)$$

If the energy gap between the ground and first excited adiabatic states is sufficiently large compared to $k_B T$, as will often be the case for localized trap states of electrons in liquids, we can neglect the thermal population of excess electron excited states, sum all of the contributions of the form in eq 51, and obtain the following expression for the diffusion constant in the limit as $k \to 0$

$$D_{ad} = \frac{1}{6}\lim_{t\to\infty}\frac{d}{dt}\int dR(0) \int dP(0) \, e^{-\beta\{P^2(0)/2M + E_0(R(0))\}} (\langle r\rangle_{\Phi_0(R(0))} - \langle r\rangle_{\Phi_0(R(t))})^2 / Z_0 \quad (54)$$

where $\langle r\rangle_{\Phi_0(R(t))} = \langle\Phi_0(R(t))|\hat{r}|\Phi_0(R(t))\rangle$ and

$$Z_0 = \int dR(0) \int dP(0) \, e^{-\beta\{P^2(0)/2M + E_0(R(0))\}} \quad (55)$$

This result was employed by Selloni et al. in their earlier work.

Appendix B. Validity of Adiabatic Ground State Dynamics Approximation

The validity of the adiabatic hypothesis was explored by integrating a set of auxiliary equations determining the evolution of the coefficient representing the electronic wave function in the instantaneous adiabatic basis set

$$\Psi(r,t;R(t)) = \sum_i c_i(t)\Phi_i(r,R(t)) \quad (56)$$

These equations are

$$i\hbar\dot{c}_k(t) = E_k(R(t))c_k(t) - i\hbar\sum_{j\neq k}\dot{R}(t)\cdot\mathbf{d}_{kj}(t)c_j(t) \quad (57)$$

where

$$\mathbf{d}_{kj}(t) = \langle\Phi_k(R(t))|\nabla_{R(t)}|\Phi_j(R(t))\rangle \quad (58)$$

is the nonadiabatic coupling vector between states k and j. In our calculations, the runs start with $c_k(0) = \delta_{k0}$, and according to eq 57, this set of values remains constant if the dynamics of the system is adiabatic (the nonadiabatic coupling vectors are all zero in this approximation). The actual occupation probabilities, $|c_k(t)|^2$, of several excited electronic states were monitored along a characteristic trajectory to investigate possible departures from pure adiabatic ground state dynamics in the overall evolution of the system.

Motivated by the approximate dynamics of Selloni et al., we employed characteristic trajectories determined by rigorous adiabatic ground state dynamics in which the Hellmann−Feynman forces are used to propagate classical evolution equations for the ions according to

$$M\frac{d^2R}{dt^2} = -\nabla_R V - \nabla_R E_0(R) \quad (59)$$

where V is the Fumi−Tosi potential describing the interactions among the ions and $E_0(R)$ is the ground state energy of the electron. The electron, however, is described quantum mechanically, and its instantaneous spectrum along the ionic trajectory is determined by solving a time-independent Schrödinger equation whose Hamiltonian, $\hat{h}$, depends parametrically on the positions of the ions.

$$\hat{h}(R)\Psi(r;R) = E(R)\Psi(r;R) \quad (60)$$

The electron−ion pseudopotentials used in our work are the same as those in refs 14, 23, 28, and 29, with the following parameters $R_+ = 3.69$ au and $R_- = 2.2$ au. Numerical tests using Lanczos diagonalization and grid methods[30] reveal that the electronic eigenvalues are converged with grids of 32^3 points.

References and Notes

(1) Hernandez, R.; Voth, G. *Chem. Phys. Lett.* **1998**, *223*, 243.
(2) Miller, W. *J. Phys. Chem. A* **2001**, *105*, 2942.
(3) Wang, H.; Sun, X.; Miller, W. *J. Chem. Phys.* **1998**, *108*, 9726.
(4) Sun, X.; Wang, H.; Miller, W. *J. Chem. Phys.* **1998**, *109*, 7064.
(5) Thoss, M.; Wang, H.; Miller, W. *J. Chem. Phys.* **2001**, *114*, 47.
(6) Zhang, S.; Pollak, E. *J. Chem. Phys.* **2003**, *118*, 4357.
(7) Poulsen, J.; Nyman, G.; Rossky, P. *J. Chem. Phys.* **2003**, *119*, 12179.
(8) Poulsen, J.; Nyman, G.; Rossky, P. *J. Chem. Phys.* **2004**, *108*, 8743.
(9) Shi, Q.; Geva, E. *J. Chem. Phys.* **2003**, *118*, 8173.
(10) Shi, Q.; Geva, E. *J. Chem. Phys.* **2004**, *120*, 10647.
(11) Shi, Q.; Geva, E. *J. Phys. Chem. A* **2003**, *107*, 9059.
(12) Shi, Q.; Geva, E. *J. Phys. Chem. A* **2003**, *107*, 9070.
(13) Ciccotti, G.; Pierleoni, C.; Capuani, F.; Filinov, V. *Comput. Phys. Commun.* **1999**, *121*, 452.
(14) Selloni, A.; Carnevali, P.; Car, R.; Parrinello, M. *Phys. Rev. Lett.* **1987**, *59*, 823.
(15) Freyland, W.; Garbade, K.; Pfeiffer, E. *Phys. Rev. Lett.* **1983**, *51*, 1304.
(16) Shao, J.; Makri, N. *J. Chem. Phys.* **2000**, *113*, 3681.
(17) Makri, N. *Phys. Rev. E* **1999**, *59*, R4729.
(18) Shao, J.; Makri, N. *J. Phys. Chem. A* **1999**, *103*, 9479.
(19) Wang, H.; Thoss, M.; Miller, W. *J. Chem. Phys.* **2000**, *112*, 47.
(20) Thoss, M.; Wang, H.; Miller, W. *J. Chem. Phys.* **2001**, *114*, 9220.
(21) Helfand, E. *Phys. Rev.* **1970**, *119*, 1.
(22) Bredig, M. *Molten Salt Chemistry*; Interscience: New York, 1964.
(23) Fois, E.; Selloni, A.; Parrinello, M. *Phys. Rev.* **1989**, *39*, 4819.
(24) Resta, R. *Phys. Rev. Lett.* **1998**, *80*, 1800.
(25) Sergi, A.; Kapral, R. *J. Chem. Phys.* **2004**, *121*, 7565.
(26) Bonella, S.; Coker, D. *Comput. Phys. Commun.* , in press.
(27) Kubo, R. *Rep. Prog. Phys.* **1966**, *29*, 255.
(28) Fois, E.; Selloni, A.; Parrinello, M.; Car, R. *J. Phys. Chem.* **1988**, *92*, 3268.
(29) Xu, L.; Selloni, A.; Parrinello, M. *Chem. Phys. Lett.* **1989**, *162*, 27.
(30) Alarvi, A. Private communication.